Tool Feed and Burr Size Influence on Wettability of Ti6Al4V Micro End-Milled

Ferreira, R., Martinelli, G. L. C., Rodrigues, A. R. and Coelho, R. T.

ABSTRACT

Surface texturing, using micro-milling, has promising applications in the industry of medical implants, since it can assist cell adhesion and thus improve osseointegration. Ti6Al4V alloy is used as implant material due to its excellent biocompatibility and high mechanical strength. However, those mechanical properties reduce machinability creating some challenges for micro-milling. The way to initially assess cell adhesion is using surface wettability, usually conducted with water. At the present work, micro-channels were machined in Ti6Al4V by micro end-milling with $500\,\mu m$ width per $50\,\mu m$ depth with $1000\,\mu m$ distant from each other. The effect of feed per tooth (fz) on wettability was analysed and some interesting relations with burrs formed on channel walls were obtained. Values of feed per tooth were 3, 6, 12 and 15 μm. Wettability results showed that slotted surface is more hydrophilic on channel direction, with contact angles around 30° to 43°. In contrast, on the perpendicular direction the surface tends to be hydrophobic with contact angles between 75° and 146°. In addition, contact angle increases (hydrophobic tendency) as feed per tooth increases (along with roughness), even on channel direction. The presence of burrs also tends to disturb wettability results. Therefore, surface wettability depends on channel direction, burr size and tool feed per tooth, as well.

Keywords: Micromilling, wettability, Ti6Al4V, surface roughness, burrs.

1 INTRODUCTION

Implants made of pure titanium or Ti6Al4V alloy, begin with conventional machining processes, such as turning and/or milling, which produce characteristic roughness and macro textures on the surface, allowing initial biological integration [9]. Micro-milling can create 3D textures to help cell adhesion, growth and proliferation, due to its characteristics [20]. However, there are still few studies relating feed per tooth and the influence of burrs on surface wettability, which is the first indication for good biological integration with human body, when applied to medical implants. Textured surface for implants has been extensively investigated lately to reduce healing time and reducing body rejection, after work published by Brånemark et al., 1969 [2]. Nowadays, the number of implants tends to increase, since life span is steadily growing and customization will be even more necessary. First studies addressing facial titanium implants in dentistry applications, between 1969 and 1980, realized that surface roughness could significantly affect healing period, which was later referred as osseointegration [1].

Shorter times for osseointegration and, consequent success in medical implants, are straightly related with cell adhesion, growing and proliferation [3]. In order to develop and stimulate those vital cell mechanisms, implant material has to match body region, roughness and textures must be adequate at macro-, micro- and nano-levels as well as surface energy [12]. After 1990 new surface treatments, after machining, such as thermal aspersion, chemical corrosion, sand blasting and anodization have contributed to improve implant surface even further. Some biomimetics process, coating with hydroxyapatit and using some bio-glasses are another ways to improve osseointegration phenomena potentially [7].

Overall, machining has been the most promising process to create textures to improve wettability and, as a consequence, biological integration. Recent publications, such as, Pratap & Patra, 2018b [15] reported that certain

Rodrigo Ferreira[1,2] ✉, Gabriel Lopes de Castro Martinelli[2], Alessandro Roger Rodrigues[2] and Reginaldo Teixeira Coelho[2]

[1]Department of Control and Industrial Processes,
Federal Institute of Pernambuco,
Av. Luís Freire, 500 - Cidade Universitária, CEP 50740-545, Recife – PE, Brazil.
[2]São Carlos School of Engineering, University of São Paulo, Brazil
E-mail: rodrigoferreira@recife.ifpe.edu.br

geometries obtained with micro ball noses can affect wettability. Wang et al., 2016 [21] shown that combining micro-milling and anodization led to better cell adhesion. In a recently published article on micro dimples, indicated that micro-textures type conical modify bacterial adhesion on the surface [8].

One of the variables indicated to assess the potential of an implant surface is wettability. The wettability may indicate how the blood will behave interacting with the material surface and its speed to promote better osseointegration [16]. Thus, when proposing the construction of topography in biomaterials at the macro, meso, micro and nanometric scales, it is necessary to investigate the wettability and its interaction with the topography and roughness [18]. Depending on the implant region, a more uniform wettability can be chosen, where the fluid spreads evenly over the surface. Another possibility is the creation of grooves so that the spreading is more effective in one direction. This effect of spreading non-uniform fluid is called wettability anisotropy [6]. Grooves on the surface of Ti6Al4V have enhanced cell adhesion compared to smooth surfaces [4]. Micro-milling can be an alternative for the manufacture of cavities (slots or channels) that promote anisotropy of wettability and have potential application in metallic implants.

The present work investigates wettability of Ti6Al4V of a surface textured with micro channels. Channels were end-milled with increasing values of feed per tooth (fz), resulting in different roughness values and some burrs at the walls. Wettability results were different, depending on roughness at the bottom of channels, on direction and on burr shape, orientation and dimensions.

2 Materials and Methods
2.1 Material and Experimental Set-Up
The material used was Ti6Al4V ELI (Extra low interstitial) titanium alloy in the annealed condition and with the presence of the α and βphases, in the form of hot-rolled sheets produced by the company TIMET, which meets the requirements found in the ASTM F136 standard. Table 1 contains the typical chemical composition of the sample, hardness (Rockwell scale) and average grain size according to ASTM E112-12.

Table 1: Typical chemical composition Ti6Al4V, grain size and hardness.

Elements	Fe	V	Al	C	O	N	Grain Size ASTM (μm)	Hardness (Rc)
Weight percent	0.18	4.08	5.98	0.009	0.11	0.009	10	30

The samples of Ti6Al4V/ELI alloy were initially prepared by gently flat-milling them into small blocks with 12 x 26 x 10 mm. A flat-end mill, diameter 20 mm, with 2 inserts, was used working with 720 rpm, fz = 0.050 mm/tooth and depth of cut 0.100 mm. Insert recommendations (R390-11 T3 08M-PL 1030) for cutting conditions.

The texture experiments were carried out on a three-axis machining centre (Hermle C800U), 500 nm positioning system (±3μ). In its spindle, a NSK Nakanishi HES 510 milling spindle was clamped. The HES 510 is capable of speeds up to 50,000 rpm continuously variable from 6,000 upwards. The speed control is the NSK controller Nakanishi Astro E500Z. Maximum tool run-out error was 2.0 μm.

Tools used were all flat-ended micro mill, solid carbide, two fluted type MS2MS D0050, diameter 500 μm (Figure 1A), multilayer coating of TiAlN (Figure 1B and 1C) and micro-grain cemented carbide substrate (grain size <0.6 μm), edge radius rε of 2.2 μm (figure 1E and 1F) measured in the OLS 4100 Olympus confocal microscope. For each test a new tool was used and its cutting-edge aspect, rake and clearance face were examined under the confocal and SEM (Figures 1D and 1E).
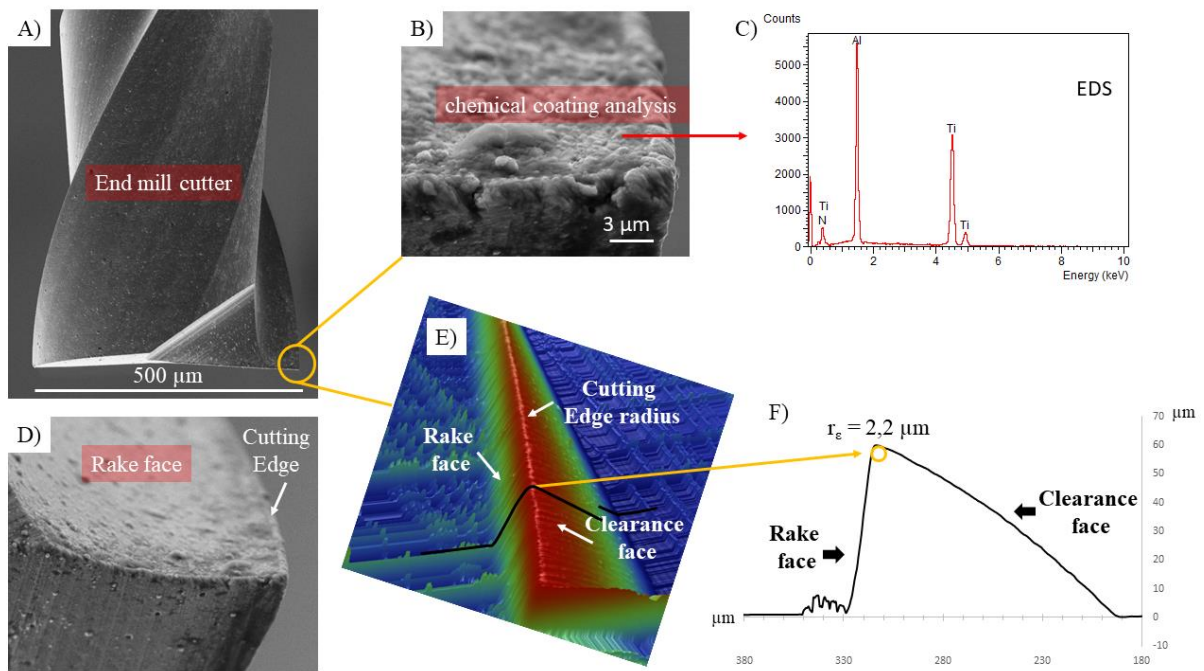
Figure 1: Characterization of the micro tool. A) Tip of the micro end mill. B) Higher magnification of the cutting edge for EDS analysis. C) Result of the EDS chemical analysis. D) Edge view by SEM. E) Confocal view to measure the edge radius. F) Measurement of the edge radius.

Initially, the machining centre went through warm up for 30 minutes before each test. The milling operations produced full slots (channels) in one-step cutting (Figure 2A). Each slot (channel) was cut on the Y-axis direction (Figure 2A) and twenty-six of them were produced, along the X-axis with 1000 μm of pitch (p) (Figure 2B). All channels were set for 50 μm depth of cut (DOC) and resulted in 500 μm wide. Values of feed per tooth (fz) used were: 3, 6, 12 and 15 μm. The cutting speed was set at 44 m/min and the speed set on the Nakanishi HES 501 fixed at 28,000 revolutions per minute (Figure 2A).
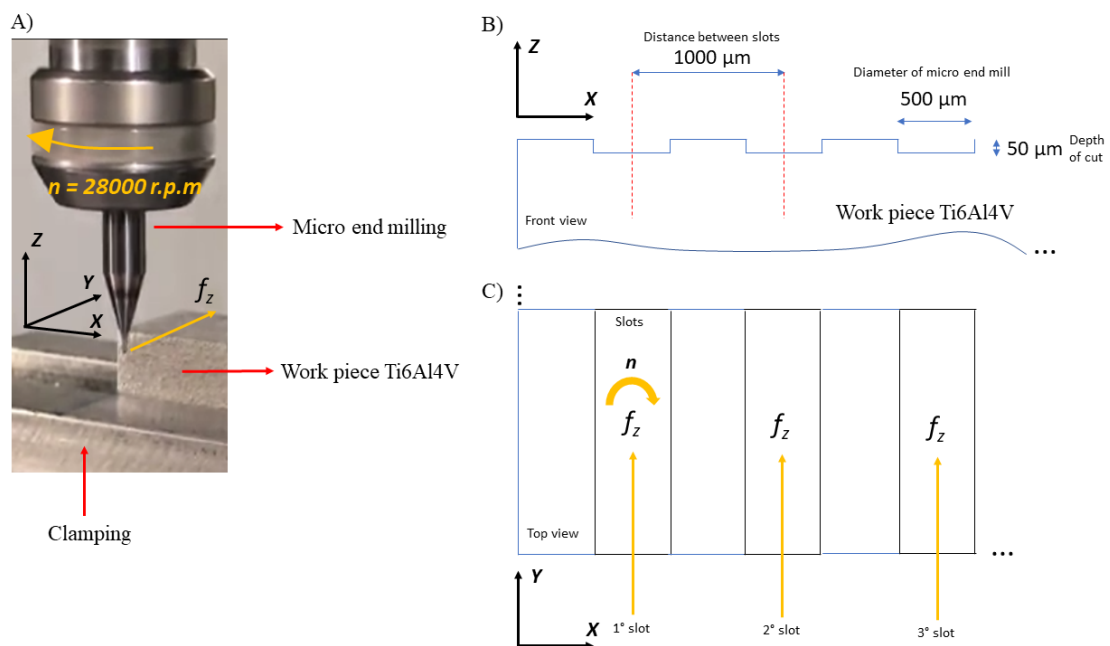

Figure 2: Configuration for slot cutting. A) General view and cutting parameters. B) Geometry of the channels in the front view and C) Top view.

2.2 Wettability

The contact angle (θ) between the liquid and solid phase is an essential parameter for inferring surface energy and evaluating the surface wettability [17]. At the present investigation, the Attension Biolin™ tensiometer, depositing 3 μl of deionized (DI) water on the surface, was the elected technique. Before the test, all samples were cleaned in an ultrasonic acetone bath. The calculation of the contact angle (θ) uses the Young-Laplace equation and was measured over 10 seconds. The baseline and vector lines between the external surface of the DI water drop and the solid surface were determined using one Attension™ software. Three measurements in different regions were performed on each sample (first channels, central ones and final ones) with an average measurement between the left and right angles (referred to as θL and θR, respectively). Images taken from the front and side of the channels served to evaluate the cases presented in Figure 3A e 3B.

The shape of the droplet and its spreading enabled the qualitative assessment of wettability in both directions, i.e., along channel direction and perpendicular to it. Some significant anisotropy in wettability was found [13]. Anisotropy of wettability is a phenomenon that is correlated to the non-uniform spreading of the drop deposited on the surface [11]. Thus, the creation of specific micro textures has a strong influence on wettability and may require analysis in different directions (Figure 3B).
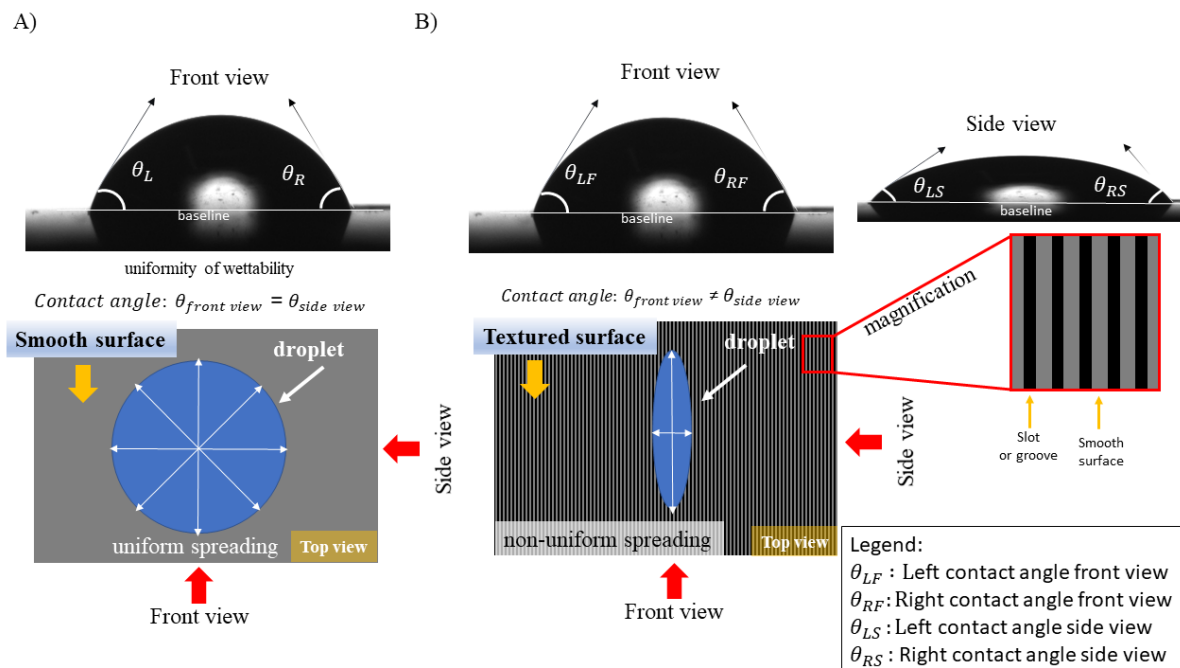
Figure 3: Analysis of wettability for smooth surfaces and with directional micro textures. A) Uniform wetting behaviour, the front and side views of wettability have similar contact angles. B) Directional micro textures with a difference in the contact angle as a function of direction. In this case, the contact angles in the front view will be different from the side view.

2.3 Superficial Characterization

Three-dimensional surface topography and area roughness (Sa) inside the channels were measured by confocal microscopy OLS 4100. Roughness measurements were taken in channels 1, 14 and 26 of all pieces manufactured in relation to the X direction at the tool entrance, middle length and at tool exit of each specific channel. Burr height measurements were performed using the Olympus LEXT 4100 software. The measurements made in the regions of interest used the ROI (Region of Interest) tool of the LEXT software (confocal microscopy), where it is possible to delimit an area. In our case we used a squared region with 200 μm of side. Scanning electron microscopy (SEM) was also performed on the LEO 440 microscope for selected cutting condition, in order to evaluate the burr formation in up and down milling locations.

3 RESULTS AND DISCUSSION

Figure 4 shows general aspects of channels obtained with different value of feed per tooth (fz) at increasing magnifications. The lowest fz value (3 μm) produced the most severe burrs on both sides of the channel, the up and down milling. It can also be noted protruding burrs inside and outside the channels. Increasing fz to 6 μm, Figure 4B, there is a considerable reduction of burrs, however they continue to protrude inside and outside the channels. When

using fz = 12 μm and 15 μm, shown in Figures 4C and 4D, burrs are at the same magnitude, but are clearly pushed outside the channels.
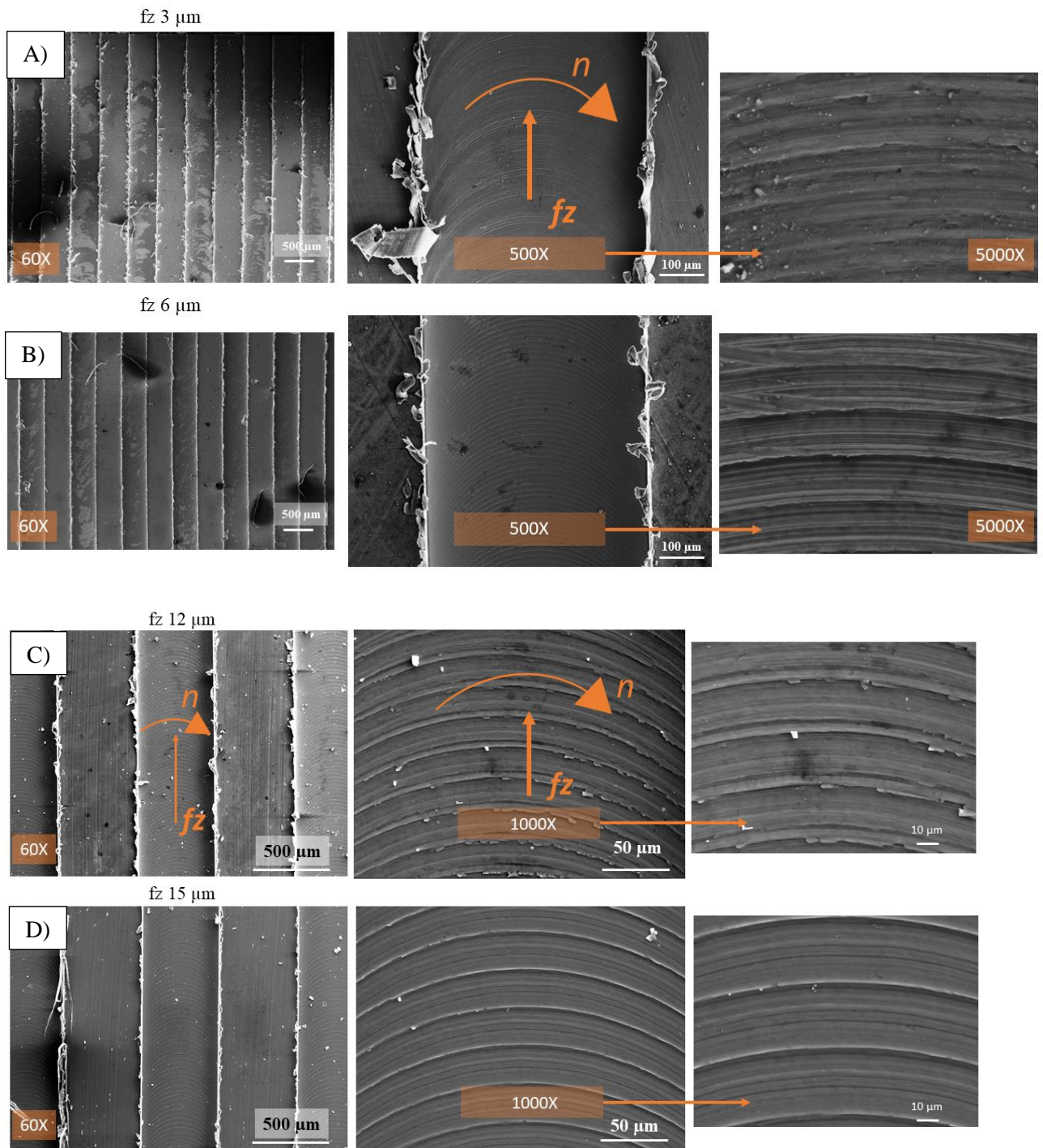
Figure 4: Scanning electron microscopy fz = 3, 6, 12 and 15 μm. A) Severe burr formation for fz = 3 μm. B) Lower burr formation for fz = 6 μm. C) Lower burrs pushed outside of the channels for fz = 12 μm. D) Lower burrs and pronounced feed marks for fz = 15 μm.

Confocal microscopy was used to evaluate 3D images of the channels e their cross sections, also assessing burrs on the walls. Figure 5A shows one channel produced with fz = 3 μm where it can be seen aspects of the burrs, such as their height. In comparison, Figure 5B, used fz = 6 μm, shows some lower burrs. On the other hand, Figures 5C and 5D show burrs bending on both sides of the walls. Figure 5E shows average heights on both walls, up and down

milling. It is noted that fz = 6 and 12 μm produced the lowest burr heights simultaneously on both walls, similarly to Thepsonthi & Özel, 2014 [19].
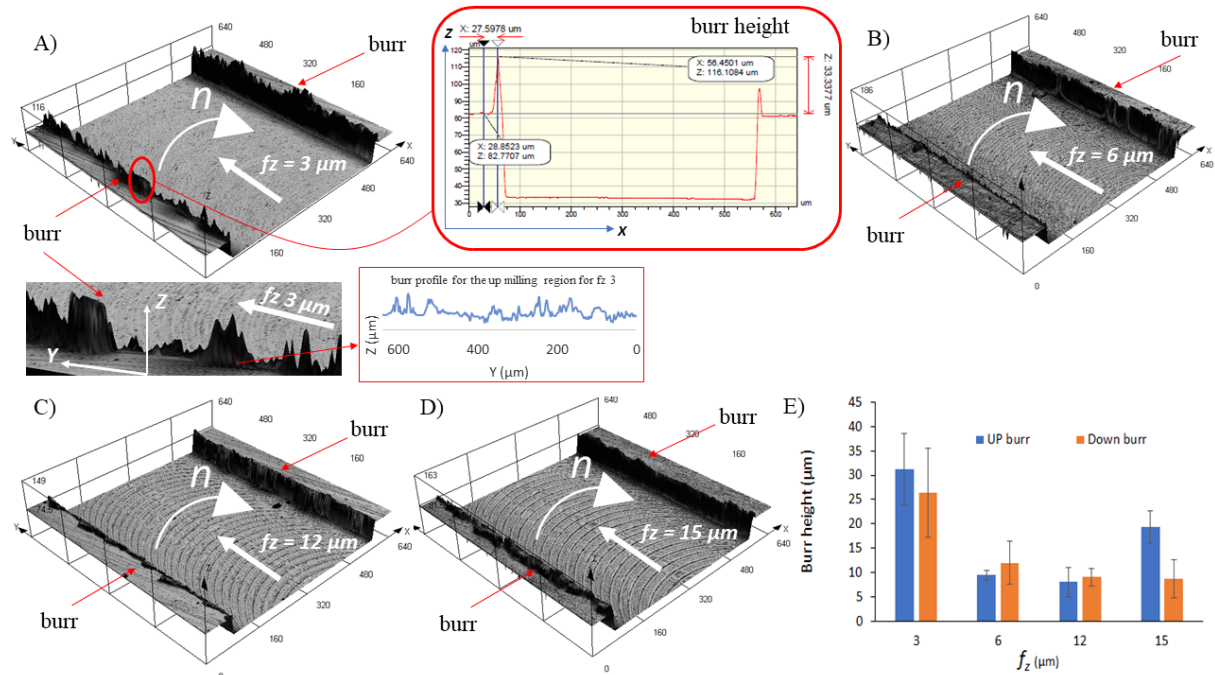

Figure 5: 3D topographies for channels manufactured with different feeds per tooth. A) fz = 3 μm. B) fz = 6 μm. C) fz = 12 μm. D) fz = 15 μm. E) Graph of burr height as a function of feed per tooth.

Figure 6 shows values of surface roughness, Sa, as a function of fz. It can be noted that roughness has a direct relation with fz, being Sa = 55 nm, the lowest value using fz = 3 μm, similar to results found by Ziberov et al.,2020 [23]. In contrast, the channel machined with fz = 15 μm reached a maximum of Sa = 321 μm, combined with a relatively high value of burr height.
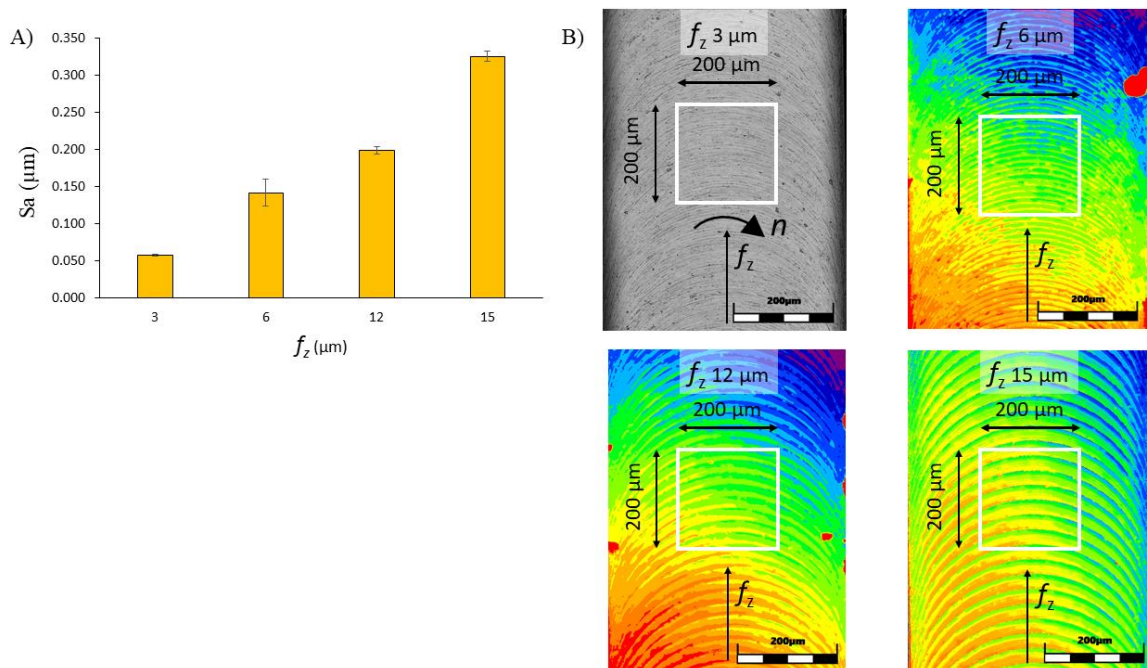
**Figure 6:** A) Values of surface roughness, Sa, as a function of feed per tooth. B) Machined surfaces images.

Figure 7 shows results of wettability measuring the contact angle as a function of fz, initially perpendicular to the channel direction. The drops of water were landed on the first channels, on the last ones and on the centrals. That intended to assess wettability all over the produced texture on the same surface.
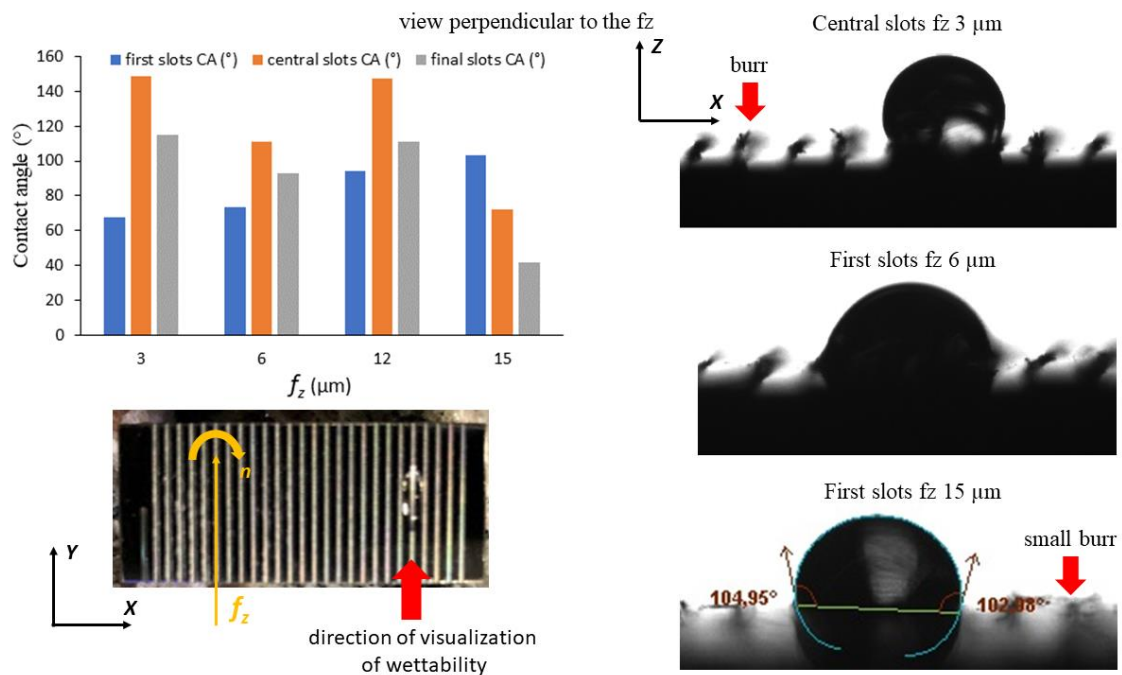
Figure 7: Contact angle depending on fz and the position of the channels. The displayed direction is perpendicular to the channel direction (front view).

Looking only on the first channels of all fz values, it can be noted an increase on contact angle (hydrophobic surfaces). That behaviour seems to follow surface roughness, which also increases with similar tendency. High values of surface roughness seem to create obstacles for water to spread and aggravated by high walls due to burr heights, especially when fz = 3 μm. Looking now at central channels only, fz = 3, 6 e 12 μm, are all hydrophobics. However, fz = 15 μm shows lower contact angle, slightly lower than 90° going to the hydrophilic direction. That cutting condition combined lower burr height and burrs pushed outside, which allowed water to spread over the channels easier than when burrs were higher. Lateral burrs, result smooth when cutting forces are higher, due to unavoidable edge wear during micro milling [5]. Although tool wear was negligible after each experiment, some edge rounding was observed, which could have been the cause for burr shape observed.

Figure 8 shows contact angle measured on the channel direction. All angles were well below 90°, resulting in hydrophilic surfaces [13]. However, contact angles moderately increase with fz, up to 12 μm. Such phenomenon is related with roughness and the surface shape left by the tool edge (see Figure 4), which creates higher obstacles for water spreading [10]. The super hydrophilic results for fz = 3 μm can be attributed to a combination of low surface roughness at the bottom of the channels, with higher walls (due to burrs heights) making easy for the water to spread along the channel and difficult to overcome the walls. Similar results were found by Yanling, Jian, & Huadong, 2018 [22] for the micro-milling of Al6061, this work showed the influence of burrs in preventing the spread of the drop deposited on the surface, generating hydrophobic surfaces in the front and side views. Such tendency did not continue with fz = 15 μm, because surface roughness at the bottom of the channels reached certain values that impeded water to spread further inside, allowing it to overflow the channels. The direction of the burrs, pushed outside for fz = 15 μm, also facilitated overflow.
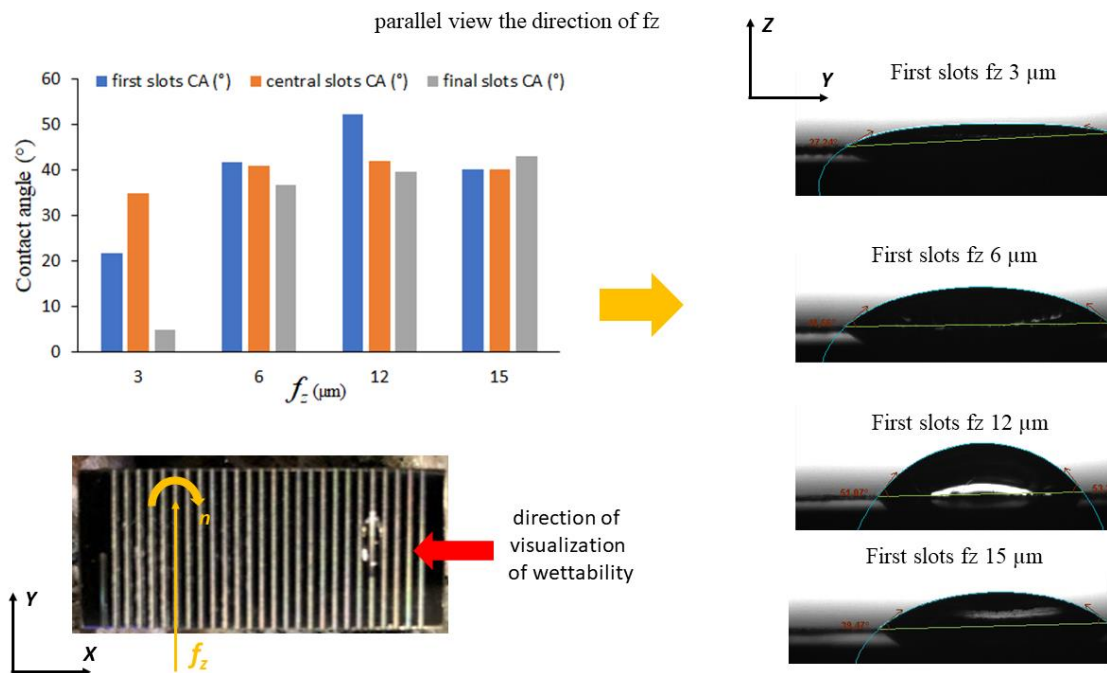
Figure 8: Contact angle as a function of fz and channel position.

Comparing contact angles measured in perpendicular directions (Figures 7 and 8), there is a notable anisotropy regarding wettability, due to the selected texture made by micro channels. Along the channels results indicate hydrophilic behaviour and perpendicular hydrophobic one [14]. Internally water molecules are attracted to each other, due to cohesion, and at the contact with air, or with a solid, they can be attracted due to adhesion. When the drop of water first touches the Ti6Al4V surface, it will search for the shape with minimum surface area possible, due to surface tension effect. The final shape of the water will result from the equilibrium of those attractions, minimizing the surface tension. Firstly, the water fills the micro channels starting from the bottom. It is easy to run on the bottom because it has to adhere to the metal and only overcome the surface roughness on the bottom and on the walls. As expected, the droplet stretches more within the micro channels.

That spreading stops when the adhesion between water molecules with air, and with metal, reaches the equilibrium with the cohesion between them internally. Such equilibrium happens at the bottom and on the walls. Simultaneously, the same equilibrium has to be achieved perpendicularly, over the micro channels, because the volume of water allows overflow. To overflow, however, enough potential energy has to be spent to reach the top of the burrs and run on the space between channels. That path seems to require much more energy because all droplets spread much less across the channels. For low roughness on the bottom and walls, when peaks and valleys are smooth, and circular in shape, water spreads easily. For roughness with the same shape, but with higher peaks and deeper valleys more energy has to be spent and water does not spread as far, before starts overflowing. If the height of the walls is lower, due to lower burrs, the water can now spread further. The shape of the burrs has also significant role to play and the spreading can be easier if burrs are pushed outside the channels, keeping the walls smoother. Therefore, anisotropy in wettability can be explained based on these considerations, according to the results found at the present work. Further investigations will also be needed, especially on the chemical compositions of the oxide layers present on the Ti6Al4V surface, after micro milling, since different oxides can have different adhesion forces on water molecules.

4 CONCLUSIONS

The study performed to investigate the influence of different values of feed per tooth (fz) on the wettability of Ti6Al4V, texturized by micro end milling, allowed the following conclusions:

1. Values of fz between 6 and 12 μm minimized burrs on the top of the walls. Those seems to be the best conditions for texturizing surfaces of medical implant. Surfaces created inside the micro channels, on bottom and walls, indicate hydrophilic behaviour, which is a good indication for biological integration;
2. Lower and higher values of fz, 3 μm and 15 μm, respectively, still produced hydrophilic surfaces inside the channels, but with excessive burrs at the top of walls, being less suitable for implants.

3. The selected texture with micro channels 50 x 500 μm, having a pitch of 1000 μm proved to be hydrophobic on the direction perpendicular to the channels. However, such texture may be useful only for specific applications on medical implants, for example in regions where directional wettability is required;
4. Modifications on the selected texture, for example, reduction of pitch, may improve the wettability and reduce anisotropy, using 6 and 12 μm to minimize burr formation.

ACKNOWLEDGEMENT

REFERENCES

1. Branemark, P. I. (1983). Osseointegration and its experimental background. *The Journal of Prosthetic Dentistry*, *50*(3), 399–410. https://doi.org/10.1016/S0022-3913(83)80101-2
2. Brånemark, P. I., Breine, U., Adell, R., Hansson, B. O., Lindström, J., & Ohlsson, A. (1969). Intra-osseous anchorage of dental prostheses: I. Experimental studies. *Scandinavian Journal of Plastic and Reconstructive Surgery and Hand Surgery*, *3*(2), 81–100. https://doi.org/10.3109/02844316909036699
3. Brett, E., Flacco, J., Blackshear, C., Longaker, M. T., & Wan, D. C. (2017). Biomimetics of Bone Implants: The Regenerative Road. *BioResearch Open Access*, *6*(1), 1–6. https://doi.org/10.1089/biores.2016.0044
4. Gui, N., Xu, W., Tian, J., Rosengarten, G., Brandt, M., & Qian, M. (2018). Fabrication and anisotropic wettability of titanium-coated microgrooves. *Journal of Applied Physics*, *123*(9). https://doi.org/10.1063/1.5020517
5. Han, J., Hao, X., Li, L., Zhong, L., Zhao, G., & He, N. (2020). Investigation on Micro-milling of Ti–6Al–4V Alloy by PCD Slotting-Tools. *International Journal of Precision Engineering and Manufacturing*, *21*(2), 291–300. https://doi.org/10.1007/s12541-019-00247-1
6. Holmes, H. R., & Böhringer, K. F. (2015). Transporting droplets through surface anisotropy. *Microsystems and Nanoengineering*, *1*(0), 1–9. https://doi.org/10.1038/micronano.2015.22
7. Jaeger, N. A. F., & Brunette, D. M. (2001). Production of Microfabricated Surfaces and Their Effects on Cell Behavior. In *Titanium in Medicine Material Science, Surface Science, Engineering, Biological Responses and Medical Applications* (Vol. 216, pp. 343–374). https://doi.org/10.1007/978-3-642-56486-4_11
8. Jain, A., Kumari, N., Jagadevan, S., & Bajpai, V. (2020). Surface properties and bacterial behavior of micro conical dimple textured Ti6Al4V surface through micro-milling. *Surfaces and Interfaces*, *21*(September), 100714. https://doi.org/10.1016/j.surfin.2020.100714
9. Kang, C. W., & Fang, F. Z. (2018). State of the art of bioimplants manufacturing: part I. *Advances in Manufacturing*, *6*(1), 20–40. https://doi.org/10.1007/s40436-017-0207-4
10. Kim, J. H., Kang, S. M., Lee, B. J., Ko, H., Bae, W. G., Suh, K. Y., … Jeong, H. E. (2015). Remote Manipulation of Droplets on a Flexible Magnetically Responsive Film. *Scientific Reports*, *5*, 1–10. https://doi.org/10.1038/srep17843
11. Kwon, D., Wooh, S., Yoon, H., & Char, K. (2018). Mechanoresponsive Tuning of Anisotropic Wetting on Hierarchically Structured Patterns. *Langmuir*, *34*(16), 4732–4738. https://doi.org/10.1021/acs.langmuir.8b00496
12. Liu, M., Zeng, X., Ma, C., Yi, H., Ali, Z., Mou, X., … He, N. (2017). Injectable hydrogels for cartilage and bone tissue engineering. *Bone Research*, *5*(November 2016). https://doi.org/10.1038/boneres.2017.14
13. Ma, C., Bai, S., Peng, X., & Meng, Y. (2013). Anisotropic wettability of laser micro-grooved SiC surfaces. *Applied Surface Science*, *284*, 930–935. https://doi.org/10.1016/j.apsusc.2013.08.055
14. Pratap, T., & Patra, K. (2018a). Direction dependent dynamic wetting of semi-hemispherical end micro-groove textured Ti-6Al-4V surface. *Surface and Coatings Technology*, *356*(July), 138–149. https://doi.org/10.1016/j.surfcoat.2018.09.037
15. Pratap, T., & Patra, K. (2018b). Fabrication of micro-textured surfaces using ball-end micromilling for wettability enhancement of Ti-6Al-4V. *Journal of Materials Processing Technology*, *262*(June), 168–181. https://doi.org/10.1016/j.jmatprotec.2018.06.035
16. Rabel, K., Kohal, R. J., Steinberg, T., Tomakidi, P., Rolauffs, B., Adolfsson, E., … Altmann, B. (2020). Controlling osteoblast morphology and proliferation via surface micro-topographies of implant biomaterials. *Scientific Reports*, *10*(1), 1–14. https://doi.org/10.1038/s41598-020-69685-6
17. Rupp, F., Gittens, R. A., Scheideler, L., Marmur, A., Boyan, B. D., Schwartz, Z., & Geis-Gerstorfer, J. (2014). A review on the wettability of dental implant surfaces I: Theoretical and experimental aspects. *Acta Biomaterialia*, *10*(7), 2894–2906. https://doi.org/10.1016/j.actbio.2014.02.040
18. Tan, J., & Saltzman, W. M. (2004). Biomaterials with hierarchically defined micro- and nanoscale structure.

Biomaterials, *25*(17), 3593–3601. https://doi.org/10.1016/j.biomaterials.2003.10.034

19. Thepsonthi, T., & Özel, T. (2014). An integrated toolpath and process parameter optimization for high-performance micro-milling process of Ti–6Al–4V titanium alloy. *International Journal of Advanced Manufacturing Technology*, *75*(1–4), 57–75. https://doi.org/10.1007/s00170-014-6102-2

20. Wan, Y., Wang, T., Wang, Z., Jin, Y., & Liu, Z. (2018). Construction and characterization of micro/nano-topography on titanium alloy formed by micro-milling and anodic oxidation. *International Journal of Advanced Manufacturing Technology*, *98*(1–4), 29–35. https://doi.org/10.1007/s00170-017-0323-0

21. Wang, T., Wan, Y., Kou, Z., Cai, Y., Wang, B., & Liu, Z. (2016). Construction of a bioactive surface with micro/nano-topography on titanium alloy by micro-milling and alkali-hydrothermal treatment. *Proceedings of the Institution of Mechanical Engineers, Part H: Journal of Engineering in Medicine*, *230*(12), 1086–1095. https://doi.org/10.1177/0954411916675382

22. Yanling, W., Jian, Y., & Huadong, Y. (2018). Superhydrophobic surface prepared by micro-milling and WEDM on aluminum alloy. *Materials Research Express*, *5*(6). https://doi.org/10.1088/2053-1591/aac6a3

23. Ziberov, M., de Oliveira, D., da Silva, M. B., & Hung, W. N. P. (2020). Wear of TiAlN and DLC coated microtools in micromilling of Ti-6Al-4V alloy. *Journal of Manufacturing Processes*, *56*(May), 337–349. https://doi.org/10.1016/j.jmapro.2020.04.082